Superfluid transition in a finite geometry: Critical ultrasonics

Saugata Bhattacharyya and J. K. Bhattacharjee
Department of Theoretical Physics, Indian Association for the Cultivation of Science, Jadavpur, Calcutta 700 032, India
(Received 19 June 1998)

The suppression of order-parameter fluctuations at the boundaries causes the ultrasonic attenuation near the superfluid transition to be lowered below the bulk value. For a confining length L, there are three characteristic lengths in the problem at a given reduced temperature t and given frequency ω. These are the correlation length ξ, the confining length L, and a dynamic length $l_d=(2\Gamma_0/\omega)^{1/z}$, where z is the dynamic scaling exponent and Γ_0 is a constant. The attenuation is a function of the two scaled variables ξ/l_d and l_d/L. We show that for $\xi \gg l_d$, the attenuation per wavelength can be processed in a manner that the data for different ω and L will collapse on a scaling plot as a function of l_d/L. For finite values of L/l_d we exhibit how the data can be plotted as a function of ξ/l_d for different values of ξ/L. We present detailed calculation for temperatures above the bulk transition temperature. These can be tested in future experiments.
[S0163-1829(98)03442-0]

I. INTRODUCTION

Critical phenomena in confined geometry[1] have been attracting a fair amount of attention of late because of the progress on the experimental front[2–9] that is making it possible to check the predictions of finite-size effects (FSE). A fair amount of this experimental effort has gone into studying the specific heat near the superfluid transition. With the bulk specific heat quite well understood and the existence of a sharp phase transition (apart from gravity rounding, which too can be removed by doing experiments in space) established, efforts have been made to study FSE. It is expected that FSE will round out the transition and hence the divergence at $T=T_\lambda$ will be removed. The specific heat will be finite and the finite value will be a function of the confining length. We will keep in mind one of the favored experimental geometries, where one takes two parallel plates separated by a distance L, much smaller than the linear dimensions of the plates. For $L \gg \xi$, the correlation length at a given temperature, the usual thermodynamic result follows. It is when $L \leqslant \xi$, that FSE dominate. Finite-size scaling suggests the existence of a scaling function, the function of ξ/L, in terms of which the theory can be cast. The specific heat $C(t,L)$ in finite geometry has the form $C(t,L) \sim t^{-\alpha} g(t^{-\nu}/L) + \text{const}$ where $\xi \sim t^{-\nu}$ and $t=(T-T_\lambda)/T_\lambda$, T_λ being the transition temperature. The function g has been calculated by various authors[10–12] and at least for $T>T_\lambda$ the calculations of $g(x)$ and the measured $g(x)$ agree reasonably well. Consequently, it makes sense to talk about a more complicated situation, one where dynamics is involved. In this paper we will discuss the ultrasonic attenuation (UA) in finite geometry. The attenuation being controlled by the frequency-dependent specific heat, our primary task will be the calculation of a temperature- and frequency-dependent specific heat in finite geometry.

The frequency dependence brings in an additional length scale. The critical fluctuations relax with a frequency ω that can be written as $\omega=\Gamma_0 k^z$, where z is the dynamic scaling exponent and Γ_0 is the Onsager constant. For the superfluid, the order-parameter fluctuations are, to a very good approximation, governed by $z=2$. The dispersion relation yields a new length scale l_d given by $l_d=(2\Gamma_0/\omega)^{1/z} \simeq (2\Gamma_0/\omega)^{1/2}$. Thus, in the finite frequency problem, there are three length scales: L, ξ, and l_d. Accordingly, we can have the following limits: (i) $L\to\infty$, (ii) $l_d\to\infty$, and (iii) $\xi\to\infty$. The first limit gives the usual ultrasonic attenuation and dispersion in the bulk. The second gives the static specific heat in the finite geometry and the third yields the ''lambda-point'' specific heat as a function of frequency and thus gives the frequency-dependent ''lambda-point'' attenuation in finite geometry.

The basis of our calculation of the attenuation is the Pippard-Buckingham-Fairbank (PBF) relation[13,14] that gives a successful account[15–17] of the critical ultrasonics in the situation where $L \gg \xi$. The PBF relation is obtained from general considerations of entropy clamping and yields, for the sound velocity $u(T,\omega)$,

$$u(T,\omega)=u_0(T_0)+u_1 C_0/C_P(T,\omega), \tag{1}$$

where $u_0(T_0)$ is the sound speed at the transition point (T_0 is the bulk T_λ for the infinite system, but is a L-dependent temperature for the finite-size system), u_1 and C_0 are constants, and $C_P(T,\omega)$ is the specific heat at finite frequency.

For the bulk case, $C_P(T,\omega=0)$ is almost divergent at $T=T_\lambda$ and $C_P(T,\omega)$ is a homogeneous function of ω and ξ. If the characteristic relaxation rate is $\Gamma_0\xi^{-z}$, then the scaling form of C_P^{bulk} is

$$C_P^{bulk}(T,\omega)=\xi^{\alpha/\nu} f\left(\frac{\omega}{\Gamma_0\xi^{-z}}\right) = \xi^{\alpha/\nu} f\left(\frac{l_d}{\xi}\right). \tag{2}$$

The exponent α is very close to zero for the superfluid transition in ^{4}He and for many practical purposes it is possible to write

$$C_P^{bulk}(T,\omega)=C\left[\ln(\Lambda\xi)+f\left(\frac{\omega}{\Gamma_0\xi^{-z}}\right)\right]$$
$$=C\left[\ln(\Lambda\xi)+f\left(\frac{l_d}{\xi}\right)\right]. \tag{3}$$

The function $f(\omega/(\Gamma_0\xi^{-z}))$ reduces to a constant for $\omega=0$ and tends to $-\ln(\omega/\Gamma_0)^{1/z}\xi$ for $\omega\gg\Gamma_0\xi^{-z}$. A one-loop calculation of the scaling function $f(\Omega)$, where $\Omega=\omega/2\Gamma_0\xi^{-z}$, was carried out and led to a successful scaling theory of the attenuation in the bulk ^{4}He near T_λ.[15–17]

In the finite-geometry situation, the specific heat will be a function of L, ξ, and l_d and we expect Eq. (3) to become

$$C_P(T,\omega,L)=C\left[\ln(\Lambda\xi)+g\left(\frac{\xi}{L},\frac{\xi}{l_d}\right)\right]. \tag{4}$$

For $L\to\infty$, g$(0,\xi/l_d)$ has to be identical to $f(\xi/l_d)$ of Eq (3). For $\omega\to 0$, we should get back the static scaling function g(ξ/L) in finite geometry and for $\xi^{-1}\to 0$, a function of l_d/L will emerge. Our primary aim will be to calculate the function g$(\xi/L,\xi/l_d)$. The single-loop calculation of the scaling function in the static limit gives a very reasonable account of the recent specific-heat data by Mehta and Gasparini.[2] One of the most important features of the scaling function is the low ξ/L limit (experimentally most easily accessible), the first departure from the thermodynamic limit, the magnitude of this departure ΔC has to be proportional to the surface (A) to volume (V) ratio and hence from purely dimensional arguments, the correction can be written as (ΔC is called the surface specific heat)

$$\Delta C=C(\xi,L)-C_\infty(\xi)=-aCA\frac{\xi}{V}, \tag{5}$$

where a is a number of $O(1)$, which can be obtained from the function $g(\xi/L)$, and C is the dimensional constant defined in Eq. (1). The agreement of this departure with the measured departure of Mehta and Gasparini is impressive.

In the present case the surface specific heat will be a generalization of Eq. (5) and can be written as

$$\Delta C(\xi,L,\omega)=C(\xi,L,\omega)-C(\xi,\omega)=-a(\xi,\omega)C(\xi)A/V, \tag{6}$$

where $a(\xi,\omega)$ is a scaling function[18] whose zero-frequency limit is $a\xi$ [see Eq. (5)] and whose general form will be calculated in Sec. II. In Sec. III, we present the full function g$(\xi/L,\xi/l_d)$, discuss the effect of finite size on the attenuation, and present a short summary.

II. THE SURFACE SPECIFIC HEAT

The complex order-parameter field $\psi_i(x)\{i=1,2\}$ will be governed by the Langevin equation

$$\dot\psi_i=-\Gamma_0\frac{\delta F}{\delta\psi_i}+N_i, \tag{7}$$

where

$$F=\int d^Dx\left[\frac{m^2}{2}\psi^2+\frac{1}{2}(\nabla\psi)^2+\frac{\lambda}{4}(\psi^2)^2\right] \tag{8}$$

and N is a Gaussian white noise. We have not shown the reversible term in the equation of motion above. The Josephson equation for the phase of the order parameter would be determining the reversible term and in principle should have a strong effect. In practice, however, because of very strong corrections to scaling the full effect of the Josephson term is not felt unless one is in an almost-critical situation. For finite-size, finite-frequency studies, it is safe to ignore the effect of this reversible term. The parameter m^2 is proportional to $T-T_\lambda$, where T_λ is the bulk transition temperature. The system is confined in one of the D directions. We call that the z direction. It is convenient to work with the Fourier transform in $D-1$ directions and the Fourier series (Dirichlet boundary conditions at $z=0$ and $z=L$ suppressing the fluctuations) in the z direction. The expansion of the time-dependent order-parameter field is

$$\psi_i(\boldsymbol{r},t)=\sum_n \psi_i(n,K,t)e^{i\boldsymbol{K}\cdot\boldsymbol{R}}\sin\left(\frac{n\pi z}{L}\right). \tag{9}$$

The equation of motion for $\psi_i(n,K,t)$ is

$$\dot\psi_i(n,K,t)=-\Gamma_0\left(m^2+K^2+\frac{n^2\pi^2}{L^2}\right)$$
$$\times\psi_i(n,K,t)+N_i+O(\psi^3). \tag{10}$$

In what follows, we will assume that all static correlations have been accounted for and $m^2=\xi^{-2}$. The specific heat is obtained as the response function corresponding to the time-dependent correlation function

$$D(\xi,L,t_{12})=\int\int\int dz_1dz_2d^{D-1}R_{12}$$
$$\times\langle\psi^2(\boldsymbol{R}_1,z_1,t_1)\psi^2(\boldsymbol{R}_2,z_2,t_2)\rangle \tag{11}$$

with $D(\xi,L,\omega)=2[\mathrm{Im}\,C(\xi,L,\omega)/\omega]$ according to fluctuation-dissipation theorem. Straightforward algebra leads to

$$C(\xi,L,\omega)=\frac{1}{L}\sum_{n=\pm1,\pm2,\ldots}\int\frac{d^{D-1}p}{(2\pi)^{D-1}}\frac{1}{\left(p^2+m^2+\frac{n^2\pi^2}{L^2}\right)}\times\frac{1}{\left(-\frac{i\omega}{2\Gamma_0}+p^2+m^2+\frac{n^2\pi^2}{L^2}\right)}$$
$$=\frac{1}{L}\sum_{n=-\infty}^{\infty}\int\frac{d^{D-1}p}{(2\pi)^{D-1}}\frac{1}{\left(p^2+m^2+\frac{n^2\pi^2}{L^2}\right)}\times\frac{1}{\left(-\frac{i\omega}{2\Gamma_0}+p^2+m^2+\frac{n^2\pi^2}{L^2}\right)}$$
$$-\frac{1}{L}\int\frac{d^{D-1}p}{(2\pi)^{D-1}}\frac{1}{(p^2+m^2)}\frac{1}{\left(-\frac{i\omega}{2\Gamma_0}+p^2+m^2\right)}. \tag{12}$$

The complete evaluation of the integral in Eq. (12) and its proper exponentiation will be studied in the next section. Here, we will restrict ourselves to the surface effect that is the first correction to the bulk $L\to\infty$ limit. In the large-L limit, in the first term on the right-hand side of Eq. (12) the sum becomes an integral and we can write a correction to $O(L^{-1})$:

$$C(\xi,L,\omega)=\int\frac{d^Dp}{(2\pi)^D}\frac{1}{(p^2+m^2)}\frac{1}{\left(-\frac{i\omega}{2\Gamma_0}+p^2+m^2\right)}-\frac{1}{2L}\int\frac{d^{D-1}p}{(2\pi)^{D-1}}\frac{1}{(p^2+m^2)}\times\frac{1}{\left(-\frac{i\omega}{2\Gamma_0}+p^2+m^2\right)}. \tag{13}$$

We work to logarithmic accuracy and hence evaluate the integrals at $D=4$ to get the functions $f(\Omega)$ and $a(\Omega)$ introduced in Eqs. (3) and (6), respectively. Note that since we are taking the logarithmic divergence for the bulk specific heat, the $C(\xi)$ in Eqs. (4) and (5) reduces the constant C of Eq. (3). The functions $f(\Omega)$ and $a(\Omega)$ are

$$f(\Omega)=\frac{1}{2}\left(\frac{1}{-i\Omega}-1\right)\ln(1-i\Omega), \tag{14}$$

$$a(\Omega)=\frac{\pi}{2}\frac{1}{-i\Omega}[\sqrt{1-i\Omega}-1], \tag{15}$$

leading to

$$C(\xi,L,\omega)=C_0\Big\{\ln\Lambda\xi-\frac{1}{4}\ln(1+\Omega^2)-\frac{1}{2\Omega}\tan^{-1}\Omega+i\left[\frac{1}{2}\tan^{-1}\Omega-\frac{1}{4\Omega}\ln(1+\Omega^2)\right]-\frac{\pi\xi}{L\Omega}(1+\Omega^2)^{1/4}\sin(\tfrac{1}{2}\tan^{-1}\Omega)-\frac{i\pi\xi}{L\Omega}\left[(1+\Omega^2)^{1/4}\cos\left(\frac{\tan^{-1}\Omega}{2}\right)-1\right]\Big\}$$
$$=C_R+iC_I, \tag{16}$$

where C_R and C_I are the real and imaginary parts of the specific heat. The specific heat is a function of the two scaling variables ξ/L and $\Omega=\omega/2\Gamma_0m^2=\xi^2/l_d^2$. For large L, consequently, we can have two different situations: $\xi,l_d\ll L$ with (i) $\xi\ll l_d$ and (ii) $\xi\gg l_d$. In case (i)

$$C(\xi,L,\omega)=C_0[\ln\Lambda\xi-\pi\xi/2L],$$

while in case (ii)

$$C(\xi,L,\omega)=C_0/2[\ln\Lambda^2l_d^2-\sqrt{2}\pi l_d/L+i(\pi/2-\sqrt{2}\pi l_d/L)].$$

Physically, case (i) corresponds to the first correction to the thermodynamic specific heat, while case (ii) deals with the first correction to the ''lambda-point'' attenuation.

We now return to Eq. (1) to find the attenuation and dispersion. The *attenuation per wavelength* is

$$\frac{\alpha\lambda}{2\pi}=\frac{u_1C_0C_I}{u_0(C_R^2+C_I^2)}, \tag{17}$$

which leads to the frequency attenuation ($\omega\gg2\Gamma_0m^2$ or $\xi\gg l_d$) as

$$\frac{\alpha\lambda}{2\pi}=\frac{\pi u_1}{u_0}\frac{1-2\sqrt{2}\left(\frac{2\Gamma_0}{\omega L^2}\right)^{1/2}}{\left[\ln\left(\frac{\omega_0}{\omega}\right)-\sqrt{2}\pi\left(\frac{2\Gamma_0}{\omega L^2}\right)^{1/2}\right]^2+\frac{\pi^2}{4}\left[1-2\sqrt{2}\left(\frac{2\Gamma_0}{\omega L^2}\right)^{1/2}\right]^2}. \tag{18}$$

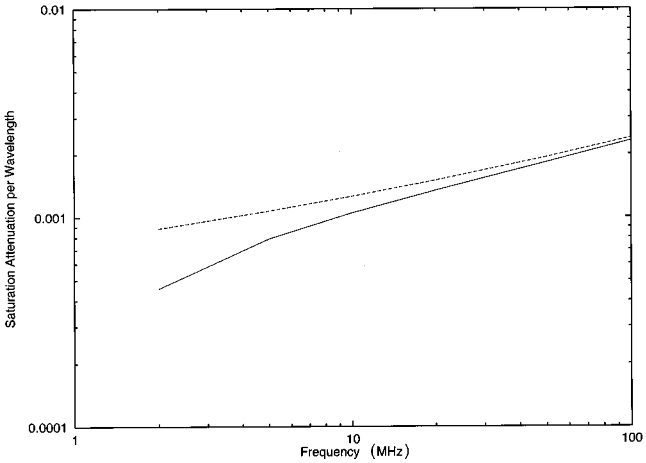

FIG. 1. Saturation attenuation is plotted against frequency. The dashed curve shows the bulk ($L\rightarrow\infty$) result whereas the solid curve shows the surface effect.

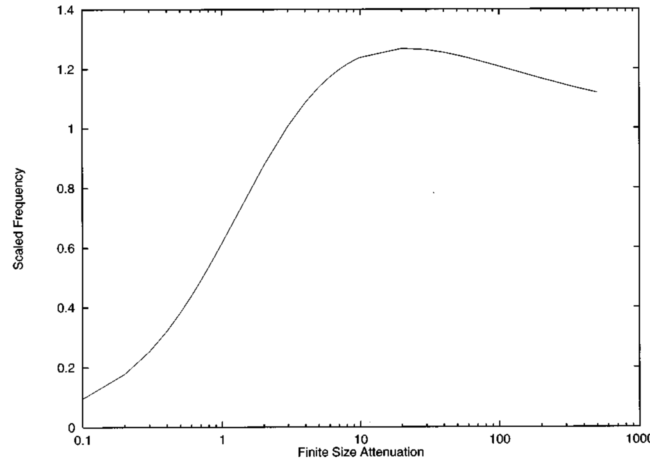

FIG. 2. Scaling plot for the finite-size attenuation per wavelength against scaled frequency in the limit $l_d \ll L$ for $l_d/L = 0.25$.

This is the *saturation attenuation* per wavelength, which does not change as the temperature is lowered further. From the known bulk behavior $\omega_0/2\pi = 30$ GHz, $\Gamma_0 = 1.2\times10^{-4}$ cm^2 sec^{-1}, $u_1/u_0 = 8/3\times10^{-2}$.

For the plate separation of 2110 Å of Mehta and Gasparini, the reduction in the attenuation due to the quenching of fluctuations is about 18% at 10 MHz and increases to 45% at 2.5 MHz. This is a large effect compared to the 4% surface effects that show up in the static measurements. For the corresponding measurement of thermal conductivity near the superfluid transition, Kahn and Ahlers[9] found that the deviation from the bulk is about 7% when the correlation length ξ equals the confining length L (in their case the radius of the pore). The effect of the finite size on the dispersion can be obtained from the real part of Eq. (1). The effect of the surface term is shown in Fig. 1.

The other sensitive part of an ultrasonic measurement is the low-frequency end ($\omega \ll 2\Gamma_0 m^2$), where for the bulk substance the attenuation per wavelength is proportional to $C_R^2\Omega/4$. The relative correction for the FSE is $1-\pi\xi/2L$, once again a larger effect than can be obtained in statics. For an easily realizable situation of $L/\xi \sim 8$, this gives a 20% reduction in the attenuation. For low values of l_d/L, the full course of the attenuation function can be seen from Eqs. (17) and (16). To obtain a close approximation to a scaling plot, we proceed by considering the ratio $\alpha\lambda/(\alpha\lambda)_{\xi\gg l_d}$ (this will be experimentally measured) and multiply by the factor $r = (C_R^2+C_I^2)/(C_R^2+C_I^2)_{\xi\gg l_d}$. The product

$$r\frac{\alpha\lambda}{(\alpha\lambda)_{\xi\gg l_d}} = \frac{C_I\left(\frac{\xi}{L},\frac{\xi}{l_d}\right)}{C_I(\xi\gg l_d)}$$

$$= \frac{2}{\pi}\,\frac{\left[\tan^{-1}\Omega - \frac{1}{2\Omega}\ln(1+\Omega^2) - 2\pi\frac{l_d}{L}\left\{\frac{(1+\Omega^2)^{1/4}\cos\left(\frac{1}{2}\tan^{-1}\Omega\right)-1}{\Omega^{1/2}}\right\}\right]}{1-2\sqrt{2}\frac{l_d}{L}}. \tag{19}$$

In Fig. 2, we show the course of this function for $l_d/L = 1/4$. For $l_d/L > 1/2\sqrt{2}$, Eq. (19) is inappropriate and so we turn to the full solution in Sec. III.

III. THE FULL SCALING FUNCTION

In this section we present the scaling function in finite geometry for all L, l_d, and ξ. To do so at the one-loop level, we exploit a result from Nicoll[19] (in the context of wave-number-depenedent specific heat). This amounts to calculating the one-loop integral $\Pi_D(L,l_d,\xi)$ in arbitrary dimension D, noting the behavior in the $L\rightarrow\infty$, $l_d\rightarrow\infty$ limit. If $\Pi_D(L\rightarrow\infty, l_d\rightarrow\infty,\xi)\sim\xi^\mu$, then the specific heat is written as $C\sim\Pi_D^{\alpha/\nu\mu}$. In our case, where α/ν is very close to zero and $\mu=1$ in $D=3$, we will evaluate the integral Π_3 in $D=3$ and write

$$C(L,l_d,\xi) = C_0 \ln \Pi_3(L,l_d,\xi), \tag{20}$$

where [see Eq. (12)]

$$\Pi_3(L,l_d,\xi)=\frac{1}{L}\sum_{n=\pm1,\pm2,\ldots}\int\frac{pdp}{\left(p^2+m^2+\frac{n^2\pi^2}{L^2}\right)\left(p^2+m^2+\frac{n^2\pi^2}{L^2}-\frac{i\omega}{2\Gamma_0}\right)}$$
$$=\frac{1}{L}\sum_{n=-\infty}^{\infty}\int\frac{pdp}{\left(p^2+m^2+\frac{n^2\pi^2}{L^2}\right)\left(p^2+m^2+\frac{n^2\pi^2}{L^2}-\frac{i\omega}{2\Gamma_0}\right)}-\frac{1}{L}\int\frac{pdp}{(p^2+m^2)\left(p^2+m^2-\frac{i\omega}{2\Gamma_0}\right)}$$
$$=\Lambda L\frac{\omega_L}{-i\omega}\left[2\ln\frac{\sinh(mL\sqrt{1-i\Omega})}{\sinh mL}-\ln(1-i\Omega)\right], \tag{21}$$

where $\omega_L=2\Gamma_0/L^2$, and Λ is scale factor.

We first explore the answer given by Eqs. (20) and (21) in the two limits where experimental data already exist. The first of these is the ultrasonic attenuation in the bulk geometry. This involves taking the limit $L\to\infty$ and we get (Λ has the dimension of inverse length)

$$C(m,\omega)=C_0\left[\ln\frac{\Lambda}{m}-\ln(1+\sqrt{1-i\Omega})\right]$$
$$=C_R+iC_I, \tag{22}$$

where

$$C_R=C_0\left[\ln\frac{\Lambda}{m}-\tfrac{1}{2}\ln\{[1+(1+\Omega^2)^{1/4}\cos(\tfrac{1}{2}\tan^{-1}\Omega)]^2+(1+\Omega^2)^{1/2}\sin^2(\tfrac{1}{2}\tan^{-1}\Omega)\}\right] \tag{23}$$

and

$$C_I=C_0\tan^{-1}\frac{(1+\Omega^2)^{1/4}\sin\left(\frac{1}{2}\tan^{-1}\Omega\right)}{1+(1+\Omega^2)^{1/4}\cos\left(\frac{1}{2}\tan^{-1}\Omega\right)}. \tag{24}$$

The attenuation per wavelength is given by Eq. (17) the right-hand side of which does not show scaling. However, to exhibit a scaling plot the measured attenuation $\alpha\lambda$ needs to be processed as follows:

$$\frac{\alpha\lambda}{(\alpha\lambda)_{T=T_c}}=\frac{4}{\pi}\frac{C_I}{C_0}\frac{(C_R^2+C_I^2)_{T=T_c}}{C_R^2+C_I^2}$$

or

$$\frac{\alpha\lambda}{(\alpha\lambda)_{T=T_c}}\frac{(C_R^2+C_I^2)}{(C_R^2+C_I^2)_{T=T_c}}=\frac{4}{\pi}\tan^{-1}\frac{(1+\Omega^2)^{1/4}\sin\left(\frac{1}{2}\tan^{-1}\Omega\right)}{1+(1+\Omega^2)^{1/4}\cos\left(\frac{1}{2}\tan^{-1}\Omega\right)} \tag{25}$$

and the right-hand side can be exhibited as a function of a scaled variable Ω. Hence, we take the experimentally measured $\alpha\lambda$ at each ω and ξ and divide by the $\alpha\lambda$ at $\xi=\infty$ for the corresponding ω. This ratio is multiplied by the factor shown in the left-hand side of Eq. (25). This factor is calculated from our theory for each ξ and ω from Eqs. (23) and (24). The resulting comparison between our theory and experiment is shown in Fig. 3 and is as good as the lowest-order ϵ-expansion calculation that had been done before.

We now discuss the other limit where experimental data exist. This is the static situation, i.e., $\omega=0$. In this case we get

$$C(\omega=0,L,\xi)=C_0\ln\left[\Lambda L\left\{\frac{\coth mL}{mL}-\frac{1}{(mL)^2}\right\}\right]. \tag{26}$$

Normalizing to the bulk value to obtain Λ and C_0, we show the comparison with available data in Fig. 4.

The success of the comparisons in the two limits where the data already exist gives us confidence in Eqs. (20) and (21). We now explore the features of the results shown in Eqs. (20) and (21) that should be probed in future experiments.

First we go to the limit $\xi\gg l_d$ with nonzero L. The result is

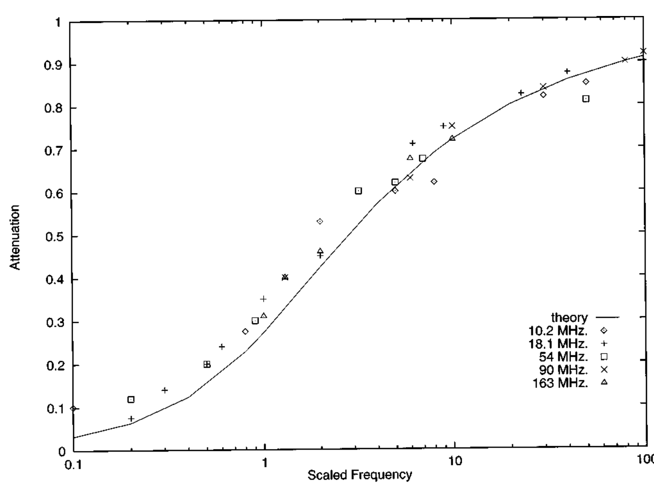

FIG. 3. Scaling plot for the frequency-dependent bulk attenuation along with the experimental data against a scaled frequency.

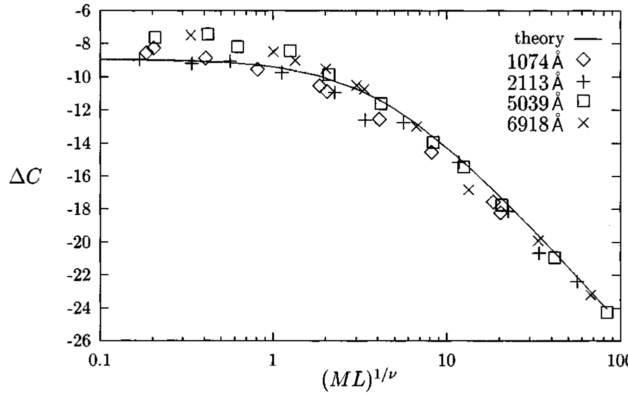

FIG. 4. $\Delta C = C(\xi,L) - C_0 \ln \Lambda L$ [Eq. (26)] plotted against $(ML)^{1/\nu}$. The solid curve refers to our theory and the data are taken from the recent experiment of Mehta and Gasparini (Ref. 2).

$$\Pi_3(L,\omega) = \Lambda L \frac{\omega_L}{-i\omega}\left[\ln\frac{\omega_L}{\omega} + \ln\left\{ \sinh^2\frac{X}{\sqrt{2}} + \sin^2\frac{X}{\sqrt{2}} \right\} + i\left\{ \frac{\pi}{2} - 2\tan^{-1}\left(\coth\frac{X}{\sqrt{2}}\tan\frac{X}{\sqrt{2}} \right) \right\} \right], \qquad (27)$$

where $X = \sqrt{\omega/\omega_L} = L/l_d$. The corresponding specific heat $C(L,l_d)$ can be written as

$$C(L,l_d) = \tilde{C}_R + i\tilde{C}_I = C_0 \ln \Lambda L \frac{\omega_L}{\omega} + \frac{1}{2} C_0 \ln\left[\left\{ 2\tan^{-1}\left(\coth\frac{X}{\sqrt{2}}\tan\frac{X}{\sqrt{2}} \right) - \frac{\pi}{2} \right\}^2 + \left\{ \ln\left(\frac{\sinh^2\frac{X}{\sqrt{2}} + \sin^2\frac{X}{\sqrt{2}}}{X^2} \right) \right\}^2 \right] + iC_0 \tan^{-1}\left[\frac{\ln\left(\frac{\sinh^2\frac{X}{\sqrt{2}} + \sin^2\frac{X}{\sqrt{2}}}{X^2} \right)}{2\tan^{-1}\left(\coth\frac{X}{\sqrt{2}}\tan\frac{X}{\sqrt{2}} \right) - \frac{\pi}{2}} \right]. \qquad (28)$$

In the limit $L \to \infty$, when $X \to \infty$, the above expression correctly reduces to $C = C_0[\ln \omega_0/\omega + i\pi/4]$. For finite L, we can construct a scaling plot for the attenuation per wavelength $\alpha\lambda$ by considering the ratio $\alpha\lambda/(\alpha\lambda)_{L\to\infty}$. This ratio is given by

$$\frac{\alpha\lambda}{(\alpha\lambda)_{L\to\infty}} = \frac{4}{\pi}\tilde{C}_I \frac{\left[\ln\frac{\omega_0}{\omega} \right]^2 + \frac{\pi^2}{16}}{\tilde{C}_I^{\,2} + \tilde{C}_R^{\,2}} = \tilde{r}^{-1}\frac{4}{\pi}\tilde{C}_I. \qquad (29)$$

By forming the quantity $\tilde{r}\alpha\lambda/(\alpha\lambda)_{L\to\infty}$, we have

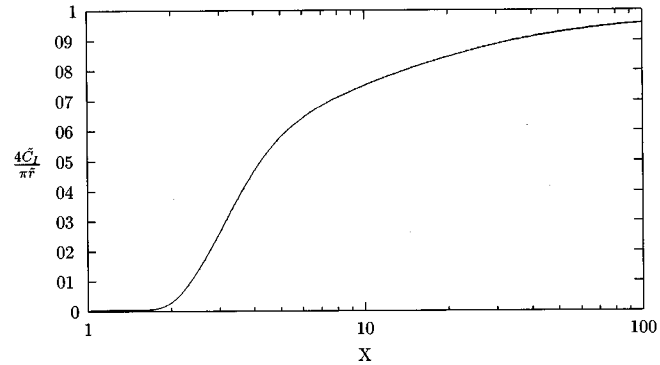

FIG. 5. Scaling plot for finite-size finite-frequency attenuation against the scaled variable X in the limit $\xi \gg l_d$.

$$\tilde{r}\frac{\alpha\lambda}{(\alpha\lambda)_{L\to\infty}} = \frac{4}{\pi}\tan^{-1}\left[\frac{\ln\left(\frac{\sinh^2\frac{X}{\sqrt{2}} + \sin^2\frac{X}{\sqrt{2}}}{X^2} \right)}{2\tan^{-1}\left(\coth\frac{X}{\sqrt{2}}\tan\frac{X}{\sqrt{2}} \right) - \frac{\pi}{2}} \right]. \qquad (30)$$

The right-hand side is a function of the scaled variable $X = L/l_d$. Thus for a given L and ω one measures the attenuation as a function of ξ and for $\xi \gg l_d$ the attenuation acquires a saturation value. For different ω and L, different saturation values are obtained. Our Eq. (20) expresses the fact that this saturation attenuation when compared to the bulk value and multiplied by a nonscaling factor $\tilde{r}$ (it is a cutoff-dependent factor), exhibits scaling behavior. The data at different ω and L collapse on a single curve when plotted against $X = \sqrt{\omega/\omega_L}$, Fig. 5. This is one of the vital predictions of our calculation.

Finally, the full specific heat needs to be written down. To do this we define the two variables

$$X_1 = mL(1+\Omega^2)^{1/4}\cos\left(\tfrac{1}{2}\tan^{-1}\Omega\right),$$
$$X_2 = mL(1+\Omega^2)^{1/4}\sin\left(\tfrac{1}{2}\tan^{-1}\Omega\right). \qquad (31)$$

The specific heat $C(m,L,\omega)$ can be written as

$$C = \tilde{\tilde{C}}_R + i\tilde{\tilde{C}}_I = C_0\left(\ln \Lambda L \frac{\omega_L}{\omega} + \frac{1}{2}\ln\left[\{2\tan^{-1}(\coth X_1 \tan X_2) - \tan^{-1}\Omega\}^2 + \left\{ \ln\left(\frac{\sinh^2 X_1 + \sin^2 X_2}{\sqrt{1+\Omega^2}\sinh^2 mL} \right) \right\}^2 \right] + i\tan^{-1}\left[\frac{\ln\left(\frac{\sinh^2 X_1 + \sin^2 X_2}{\sqrt{1+\Omega^2}\sinh^2 mL} \right)}{2\tan^{-1}(\coth X_1 \tan X_2) - \tan^{-1}\Omega} \right] \right). \qquad (32)$$

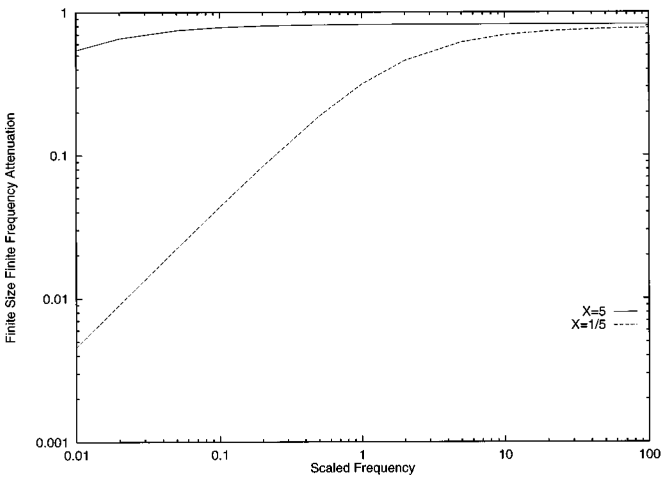

FIG. 6. Scaling plot for the finite-size finite-frequency attenuation as a function of the scaled variable Ω for two different values of l_d/L. The solid curve refers to $l_d/L=0.2$ and the dashed curve refers to $l_d/L=5.0$.

The attenuation per wavelength is given by a relation of the form shown in Eq. (17) that becomes in this case

$$\frac{\alpha\lambda}{2\pi}=\frac{u_1 C_0 \tilde{\tilde{C}}_I}{u_0(\tilde{\tilde{C}}_R{}^2+\tilde{\tilde{C}}_I{}^2)}. \tag{33}$$

The best way of exhibiting the measured attenuation (as a function of t, ω, L) would be to form the ratio of the above $\alpha\Lambda$ with the corresponding value for $\Omega\gg 1$, i.e., $\xi\gg l_d$. We find

$$\frac{\alpha\lambda}{(\alpha\lambda)_{\Omega\gg1}}=\frac{\tilde{\tilde{C}}_I}{\tilde{C}_I}\,\frac{\tilde{C}_R{}^2+\tilde{C}_I{}^2}{\tilde{\tilde{C}}_R{}^2+\tilde{\tilde{C}}_I{}^2}=\frac{1}{\tilde{\tilde{r}}}\,\frac{\tilde{\tilde{C}}_I}{\tilde{C}_I}$$

leading to

$$\tilde{\tilde{r}}\frac{\alpha\lambda}{(\alpha\lambda)_{\Omega\gg1}}=\frac{\tilde{\tilde{C}}_I}{\tilde{C}_I}. \tag{34}$$

In Fig. 6, we exhibit the right-hand side as a function of Ω for two different values of l_d/L, namely, 1/5 and 5. For the smaller system, the saturation of $\alpha\lambda/(\alpha\lambda)_{\Omega\gg1}$ occurs more slowly as expected. In Figs. 5 and 6, we have exhibited our main findings. The experiments, when carried out in the future will measure $\alpha\lambda$ at various values of ξ, ω, and L. Exhibiting the data will be facilitated by following the prescriptions in Eqs. (30) and (34). In each case, it is recommended that the data be presented as a ratio and multiplied by scale factor $(\tilde{r},\tilde{\tilde{r}})$ that has been calculated.

We end our discussion by pointing out that plate separation of the order of 1000 Å, which is feasible for static measurements, may not be appropriate for sound attenuation measurements. The limitation could come from how small the transducers can be. To accommodate the transducers, the plate separation may have to be of the order of 1 to 10 μm. For $L=1$ μm (10^4 Å) and for a frequency $\omega=1$ Mhz, corresponding to $l_d\simeq 650$ Å it should be possible to explore the whole range of ξ and test the veracity of Eq. (19). Future generation experiments should be able to verify Eqs. (33) and (34).

ACKNOWLEDGMENTS

One of the authors (S.B.) would like to thank the C.S.I.R, India, for providing partial financial support and Dr. Manabesh Bhattacharya for his help and encouragement.

[1] For a review, see V. Dohm, Phys. Scr. **T49**, 46 (1993).

[2] S. Mehta and F. M. Gasparini, in *Proceedings of the Twenty-first International Conference on Low-Temperature Physics* [Czech. J. Phys. **46**, Suppl. S1, 173 (1996)]; Phys. Rev. Lett. **78**, 2596 (1997).

[3] T. P. Chen and F. M. Gasparini, Phys. Rev. Lett. **40**, 331 (1970).

[4] F. M. Gasparini, G. Agnolet, and J. D. Reppy, Phys. Rev. B **29**, 138 (1984).

[5] I. Rhee, F. M. Gasparini, and D. J. Bishop, Phys. Rev. Lett. **63**, 410 (1989).

[6] J. A. Nissev, T. C. P. Chui, and J. A. Lipa, J. Low Temp. Phys. **92**, 393 (1993).

[7] M. Coleman and J. A. Lipa, in *Proceedings of the Twenty-first International Conference on Low-Temperature Physics* (Ref. 2), p. 183.

[8] G. Ahlers and R. V. Duncan, Phys. Rev. Lett. **61**, 846 (1988).

[9] A. M. Kahn and G. Ahlers, Phys. Rev. Lett. **74**, 944 (1995).

[10] W. Huhn and V. Dohm, Phys. Rev. Lett. **61**, 1368 (1988).

[11] R. Schmolke, A. Wacker, V. Dohm, and D. Frank, Physica B **165-166**, 575 (1990).

[12] P. Sutter and V. Dohm, Physica B **194-196**, 614 (1994).

[13] A. B. Pippard, Philos. Mag. **1**, 473 (1956).

[14] M. J. Buckingham and W. M. Fairbank, in *Progress in Low Temperature Physics*, edited by C. J. Gorter (North-Holland, Amsterdam, 1961), Vol. III, p. 80.

[15] R. A. Ferrell and J. K. Bhattacharjee, Phys. Rev. Lett. **44**, 403 (1982).

[16] R. A. Ferrell and J. K. Bhattacharjee, Phys. Rev. B **23**, 2434 (1981).

[17] J. Pankert and V. Dohm, Phys. Rev. B **40**, 10 856 (1989).

[18] S. Bhattacharyya and J. K. Bhattacharjee, J. Phys. A Lett. **31**, 575 (1998); Europhys. Lett. **43**, 129 (1998).

[19] J. F. Nicoll, Phys. Lett. **80A**, 317 (1980).